Research article

Calcium-mediated transductive systems and functionally active gap junctions in astrocyte-like GL15 cells

Maria A Mariggio*[1], Giovanna Mazzoleni[2], Tiziana Pietrangelo[1], Simone Guarnieri[1], Caterina Morabito[1], Nathalie Steimberg[2] and Giorgio Fano[1]

Address: [1]Dipartimento di Scienze del Farmaco, Laboratorio di Fisiologia Cellulare, Università "G. D'Annunzio", I-66013 Chieti and and [2]Sezione di Patologia Generale ed Immunologia, Dipartimento di Scienze Biomediche e Biotecnologie, Facoltà di Medicina e Chirurgia, Università di Brescia, I-25123 Brescia, Italy

E-mail: Maria A Mariggio* - mariggio@unich.it; Giovanna Mazzoleni - mazzolen@med.unibs.it; Tiziana Pietrangelo - tiziana@unich.it; Simone Guarnieri - guarnie@unich.it; Caterina Morabito - c.morabit@unich.it; Nathalie Steimberg - steimber@med.unibs.it; Giorgio Fano - fano@unich.it

*Corresponding author

Published: 17 May 2001

BMC Physiology 2001, **1**:4

Received: 11 April 2001
Accepted: 17 May 2001

This article is available from: http://www.biomedcentral.com/1472-6793/1/4

Abstract

Background: It has been proposed that GL15, a human cell line derived from glioblastoma multiforme, is a possible astroglial-like cell model, based on the presence of cytoplasmic glial fibrillary acidic protein.

Results: The aim of this work was to delineate the functional characteristics of GL15 cells using various experimental approaches, including the study of morphology, mechanism of induction of intracellular Ca^{2+} increase by different physiological agonists, and the presence and permeability of the gap-junction system during cell differentiation.

Immunostaining experiments showed the presence and localization of specific glial markers, such as glial fibrillary acidic protein and S100B, and the lack of the neuronal marker S100A. Notably, all the Ca^{2+} pathways present in astrocytes were detected in GL15 cells. In particular, oscillations in intracellular Ca^{2+} levels were recorded either spontaneously, or in the presence of ATP or glutamate (but not KCl).

Immunolabelling assays and confocal microscopy, substantiated by Western blot analyses, revealed the presence of connexin43, a subunit of astrocyte gap-junction channels. The protein is organised in characteristic spots on the plasma membrane at cell-cell contact regions, and its presence and distribution depends on the differentiative status of the cell. Finally, a microinjection/dye-transfer assay, employed to determine gap-junction functionality, clearly demonstrated that the cells were functionally coupled, albeit to varying degrees, in differentiated and undifferentiated phenotypes.

Conclusions: In conclusion, results from this study support the use of the GL15 cell line as a suitable *in vitro* astrocyte model, which provides a valuable guide for studying glial physiological features at various differentiation phases.

Background

Astrocytes are the most abundant cell type of the central nervous system, where they are closely involved in the modulation of the activity of neuronal components. Astrocytes play a pivotal role in several physio-pathological brain events that involve the synthesis and secretion of neurotrophic growth factors [1]. In addition, it has been shown that neurotrophin-mediated signalling may not be the only mechanism involved in astrocyte-neuron interactions. In fact, the presence of specific intercellular connections (gap junctions) between these two cell populations, which allow direct and selective cell-to-cell exchange of chemical signals (ions, small metabolites), may represent an additional, rapid and unique way for astrocytes to communicate with each other and to interact with adjacent neurons [2].

In mammalian astrocytes, extracellular physiological agonists are able to increase the concentration of intracellular Ca^{2+} ($[Ca^{2+}]_i$) via voltage-dependent channels or controlled release from internal stores (via inositol triphosphate receptors and/or ryanodine receptors) [3, 4, 5]. This is one of the most utilised mechanisms for modulating astrocyte functions. However, Ca^{2+} waves, which are transmitted from cell to cell via gap junctions (gjs), are thought to be important for co-ordination of astroglial function [6, 7, 8]. The genesis and propagation of Ca^{2+} waves were originally observed in brain-derived cell populations in culture and, more recently, this event has also been demonstrated in more integrated systems, such as brain slice preparations [4, 9] and living rat brain [10]. In spite of the large number of contributions published in the last decade, the mechanism(s) involved in the genesis and propagation of Ca^{2+} waves are not yet clear [11]. Moreover, there is insufficient data from *in vivo* experiments, especially those on human astrocytes.

About ten years ago, the GL15 cell line was established from human glioblastoma multiforme [12]. GL15 cells were characterised as an astroglial-like cell line by the study of the cell karyotype and immunohistochemical and cytogenetic demonstration of glial fibrillary acidic protein (GFAP) expression [12]. Moreover, other biochemical properties peculiar to astroglials were found in the GL15 cellular population that confirmed their astroglial origin; for example, expression of glutamine synthetase, taurine transport, transforming growth factor receptor expression and interleukin-induced apoptosis [13, 14, 15, 16]. Although the data derived from the previous studies support the presence of an astroglial phenotype, as yet no determination has been made concerning the main physiological characteristics of the GL15 cells in relation to their differentiation.

Therefore, we decided to focus our attention on one of the most important aspects of astrocyte physiology: the mechanism(s) of cell communication. Considering that *in vivo* astrocytes are capable of cellular communication both via membrane surface receptor-operated systems and/or gjs between two neighbouring cells, the investigation of the presence and activity of these mechanisms is fundamental in proposing GL15 cells to be an *in vitro* model of astrocytes.

For these reasons, we define the characteristics of this model by analysing some morphological aspects, the mechanism of $[Ca^{2+}]_i$ increase induced by different extracellular physiological agonists and the expression and functional capacity of the gjs system in relation to the differentiative pathway.

Results

Morphological analysis

Undifferentiated GL15 cells have a heterogeneous morphology. Figure 1 shows confocal microscopy images of the different typologies of these cells. Fluorescent markers were used to make evident the structural characteristics of these cells, namely, the microtubule array of the cytoskeleton (Paclitaxel-Bodipy, green fluorescence) (Fig. 1A), the nuclear structure and the mitochondria network (Propidium Iodide, red fluorescence, and Mitotracker-Green488, green fluorescence, respectively) (Fig. 1B), and the F-actin organization (Phalloidin-Alexa594, red fluorescence) (Fig. 1C). These data made it clear that cytoskeleton organization and lobate nuclei were characteristic of each cellular element, confirming the population heterogeneity.

Replacement of the 10% FCS in the culture medium with 2% HS, in order to induce cell differentiation, caused the GL15 cell growth rate to slow and apoptosis to be triggered. Therefore, the differentiation phase was completed within 9-12 days. The percentage of apoptotic and dividing nuclei (assayed by staining with the fluorescent nuclear probe DAPI) present during the differentiation period (0-12 days) are reported in Table 1. The percentage of mitotic cells fell sharply from 9-12% (0-3 days) to 1-2% after 12 days, whereas the presence of apoptotic nuclei increased during the first 3 days (from 5% to 16%) and regained its initial value at day 12 of differentiation. The characteristics of the proliferation rate and apoptosis process in GL15 cells can also be correlated with the morphological analysis carried out over the same time interval. In particular, in 10% FCS-supplemented DMEM or after only 1-2 days in 2% HS-supplemented medium, the cells, characterised by a high proliferation rate (see the mitotic nuclei percentage in Table 1), showed an extreme morphological heterogeneity with elongated, fibroblast-like cells in a range of sizes together with larger, flat and more polygonal-shaped elements

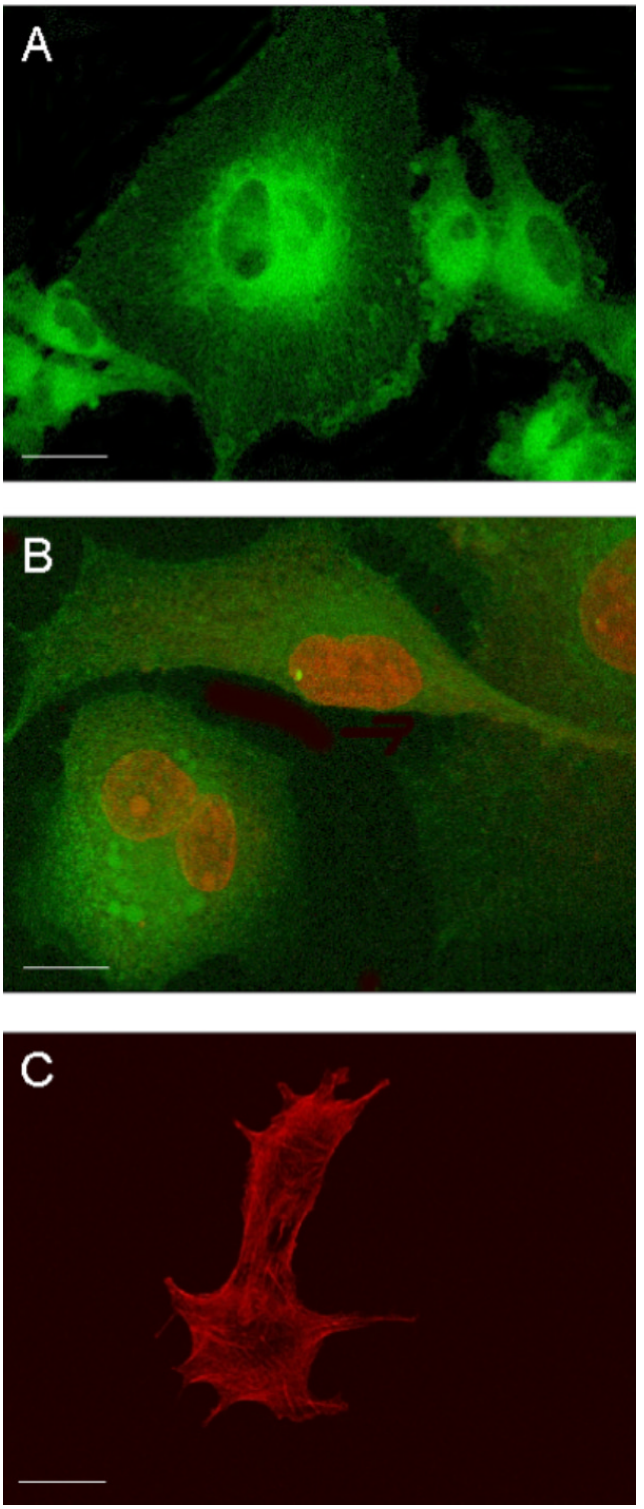

Figure 1
Confocal images of different GL15 cell typology. Panel A: an overlay of single-section images of cells, stained with Paclitaxel-Bodipy (green fluorescence), shows tubulin organization in the cytoskeleton; panel B: an overlay of single-section images of cells, double-stained with Mitotracker-Green488 and Propidium Iodide, highlights mitochondrial network (green fluorescence) and lobate nuclei (red fluorescence); panel C: single median-section image of two cells, stained with Phalloidin-Alexa594 (red fluorescence), shows actin organization in the cytoskeleton. Bar = 25 μm.

Table 1: GL15 nucleus morphology analysis during differentiation phases

Nucleus typology	Differentiation days				
	0	3	6	9	12
normal	86 ± 10.2	72 ± 8.3	91 ± 7.5	87 ± 9.4	94 ± 11.3
mitotic	9 ± 2.3	12 ± 2.1	2 ± 0.8	2 ± 1.5	1 ± 0.9
apoptotic	5 ± 1.5	16 ± 3.1	7 ± 2.6	8 ± 2.3	5 ± 1.9

Data derived from DAPI-stained nuclei (see Materials and Methods) observed using a fluorescence microscope. Each value represents the mean ± s.d. of the percentage of nuclei with different morphology: regular lobate nuclei (normal), two distinct nuclear lobes (mitotic) and enriched pluri-lobate nuclei (apoptotic). During selected differentiation times (0, 3, 6, 9 and 12 days), the percentages were calculated from values derived from five randomly selected fields each containing about 50-60 cells on slices, in duplicate for each sample.

(Fig. 2A). In contrast, the 10-day confluent cells cultured in the presence of 2% HS showed apparent homogeneous morphology. Most of the cells were of small size with a regular, round shape (Fig. 2B); the extremely rare mitoses and numerous thin cell elongations, which form a sort of web within the culture, were strongly suggestive of resting or differentiated cells (Fig. 2B).

To better define the glial features of GL15 cells, we also tested for the presence of specific astrocytic markers (GFAP and S100B). Immunolabelling for GFAP and the use of confocal microscopy highlighted, in both undifferentiated and differentiated phenotypes, a diffuse expression of the protein in the cytoplasmic compartment (Figs 2C and 2D). Under the same conditions, we also tested the expression of S100A and S100B, two Ca^{2+}-binding proteins characteristically distributed in the central nervous system, but with different modalities: S100A is predominantly expressed in neurons, whereas S100B is normally expressed in and secreted by astroglial cells [17]. Both undifferentiated and differentiated GL15 cells were S100B-positive (Figs 2E and 2F, respectively). A marked distribution of S100B was found in the perinuclear area, above all in the differentiated phenotype (Fig. 2F), and the undifferentiated phenotype also showed a diffuse cytoplasmic localization (Fig. 2E). In contrast, S100A was not detected (data not shown). This result is particularly significant, because it indicates a specific astroglial feature of the GL15 line.

$[Ca^{2+}]_i$ levels

We also studied the membrane activating systems of GL15 cells by analysing, in single cells, the $[Ca^{2+}]_i$ variations triggered by extracellularly applied stimuli for which the concentration and effect on astroglial cells are well known. Figures 3, 4, 5 and 6 show the temporal analysis of single cell $[Ca^{2+}]_i$ variation expressed as normalized fluorescence values (see Materials and Methods).

The main graph in Fig. 3 shows the repetitive Ca^{2+} variations induced by 50 mM KCl that were found in 100% of the differentiated cells (Δ of $[Ca^{2+}]_i$ increase = 7 ± 2; n = 60). In the undifferentiated GL15 cells, only 70% of the cell population responded to KCl, with $[Ca^{2+}]_i$ variations showing a kinetic shape similar to that observed for the differentiated ones, but with a lower amplitude (Δ of $[Ca^{2+}]_i$ increase = 1 ± 0.5; n = 47; trace in the box). We also tested the cell response to glutamic acid (L-glu) and ATP which, like other physiological extracellular signals, induce $[Ca^{2+}]_i$ variation in astroglial cells via membrane-receptor systems. Starting from a concentration of 300 μM, L-glu induced in 83% of undifferentiated cells a rapid increase in $[Ca^{2+}]_i$ that regained the basal value within 4 minutes (Δ of $[Ca^{2+}]_i$ increase from 1 to 3.5; n = 60) (Fig. 4A). In contrast, 100% of differentiated cells were responsive to 300 μM L-glu (n = 70), but with different kinetics and time-course. In fact, as shown in Fig. 4B, three different Ca^{2+} pathways, with the same probability percentage, were recorded in this phenotype: i) a single transient $[Ca^{2+}]_i$ spike, ii) a $[Ca^{2+}]_i$ variation with a shape similar to that observed in the undifferentiated phenotype, and iii) $[Ca^{2+}]_i$ oscillations. Another physiological stimulus able to trigger an intracellular Ca^{2+} response in GL15 cells was the presence of 200 μM ATP in the medium. While this purinergic agonist did not induce $[Ca^{2+}]_i$ variation in the undifferentiated population (0 responsive cells out of 53 tested cells; data not shown), in the 10-day low serum-treated cells 200 μM ATP caused single Ca^{2+} spikes or oscillations in 50% (n = 69) of the stimulated cells, with a ratio of 2:1 between the two possibilities (Figs 5A and 5B). Another important observation is that the different types of $[Ca^{2+}]_i$ variation are derived from different involvements of intracellular

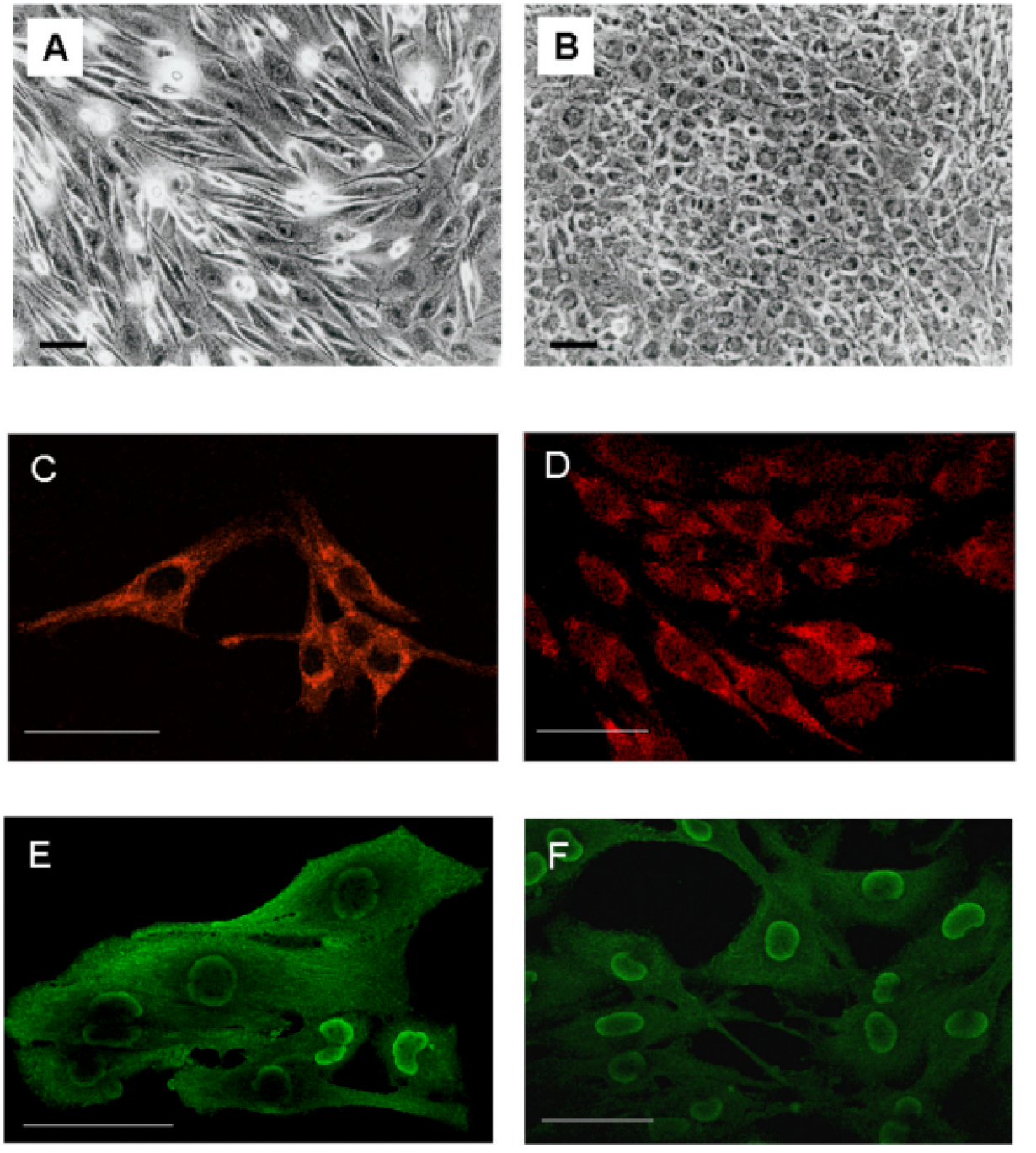

Figure 2
GL15 phenotypes. Panels A and B represent, respectively, phase-contrast images of sub-confluent undifferentiated cells, grown in D-MEM containing 10% FCS, and differentiated cells incubated for 10 days in D-MEM supplemented with 2% HS. Panels C and D show, respectively, confocal GFAP localization in undifferentiated and differentiated GL15 cells immunostained with Cy3-conjugated anti-GFAP antibody (red fluorescence). The images (single focal plane at intermediate cell section) show no detectable difference in GFAP distribution between the two phenotypes. Panels E and F visualize, in undifferentiated and differentiated GL15 cells respectively, single focal plane at intermediate cell section images showing S100 expression in cells immunostained with OregonGreen-conjugated anti-S100B antibody (green fluorescence). The fluorescence signal indicates that S100B is localized in the perinuclear area. This finding is more evident in the differentiated phenotype. The same samples were also stained with TexasRed-conjugated anti-S100A, but no red fluorescent emission was detected. Bar = 50 μm.

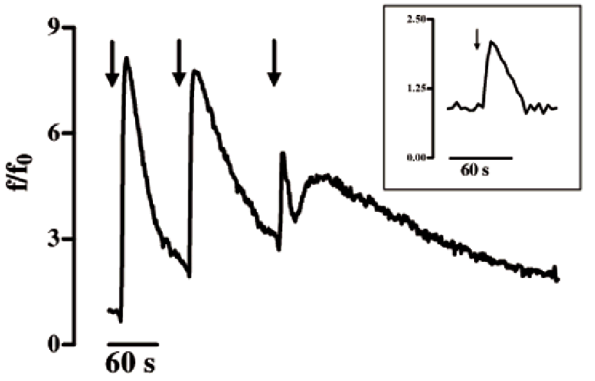

Figure 3

KCl-evoked Ca^{2+} spikes in GL15 cells. The graph shows the trace of intracellular Ca^{2+} variations in a single cell responding to extracellular 50 mM KCl pulses (arrows). The solid trace represents the $[Ca^{2+}]_i$ variations found in 100% (n = 60) of the differentiated tested cells. The trace in the box represents the $[Ca^{2+}]_i$ variations found in 70% (n = 47) of the undifferentiated cells. Time (s=seconds) is indicated on the abscissa; the ordinate gives the normalized fluorescence value (f/f_0).

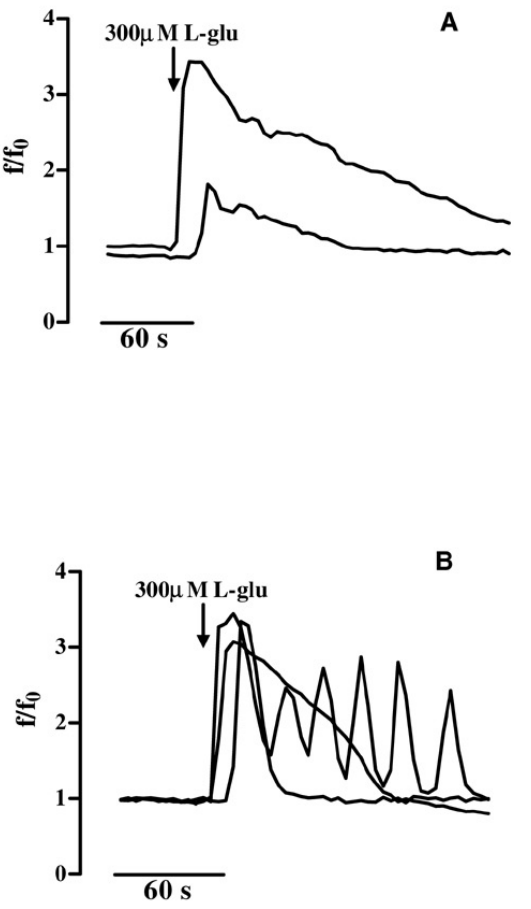

Figure 4

Temporal analysis of $[Ca^{2+}]_i$ variations induced by L-glutamic acid in GL15 phenotypes. Of the undifferentiated cells (n = 60), 83% were responsive to addition of 300 μM L-glutamic acid (L-glu) (arrow) with the same kinetics although with different amplitudes (A). In panel B the traces represent the three equally probable $[Ca^{2+}]_i$ kinetics (fast increase and fast decay; fast increase and slow decay; Ca^{2+} waves) recorded in 100% (n = 70) of differentiated cells tested. Time (s=seconds) is indicated on the abscissa; the ordinate gives the normalized fluorescence value (f/f_0).

Ca^{2+}-stores. In fact, in 18% of the differentiated cells that showed Ca^{2+} oscillations, 200 μM ATP almost completely emptied the intracellular Ca^{2+}-stores. This was confirmed by the further addition of thapsigargin, a well-known blocker of internal store Ca^{2+}-pumps [18], which caused a slight increase in $[Ca^{2+}]_i$ (Fig. 5B). In contrast, if the same thapsigargin concentration was added to the cell that responded to the presence of 200 μM ATP with a single spike, the alkaloid induced a large and sustained increase in Ca^{2+} (Fig. 5A).

Another distinctive aspect of this cell line was the presence of spontaneous Ca^{2+} variations, a phenomenon frequently observed in cells of astroglial origin. GL15 cells showed at least three different kinetics of Ca^{2+} oscillations: i) single transient variation (Fig. 6A) ii) low frequency oscillations (Fig. 6B) and iii) high frequency oscillations (Fig. 6C) (see also additional data: Movie 1 for the original data used to perform this analysis). Spontaneous Ca^{2+} variations were observed in both GL15 phenotypes. The phenomenon seemed to be independent of the presence of external Ca^{2+}, because spontaneous $[Ca^{2+}]_i$ variations were detectable both in the presence of 1.8 mM extracellular Ca^{2+} and in Ca^{2+}-free external medium containing 5 mM EGTA (data not shown). To quantify this phenomenon, we tested more than 200 undifferentiated and differentiated cells; among these, 50% of each cell population seemed to be able to prime spontaneous intracellular Ca^{2+} movements. However, considering the variability of the genesis of spontaneous $[Ca^{2+}]_i$ oscillations, this cell percentage could be even higher.

Gap-junction analysis

The complex process of astrocytic Ca^{2+} signalling involves not only the inner cellular pathway (information flow throughout the sub-cellular compartments) and the

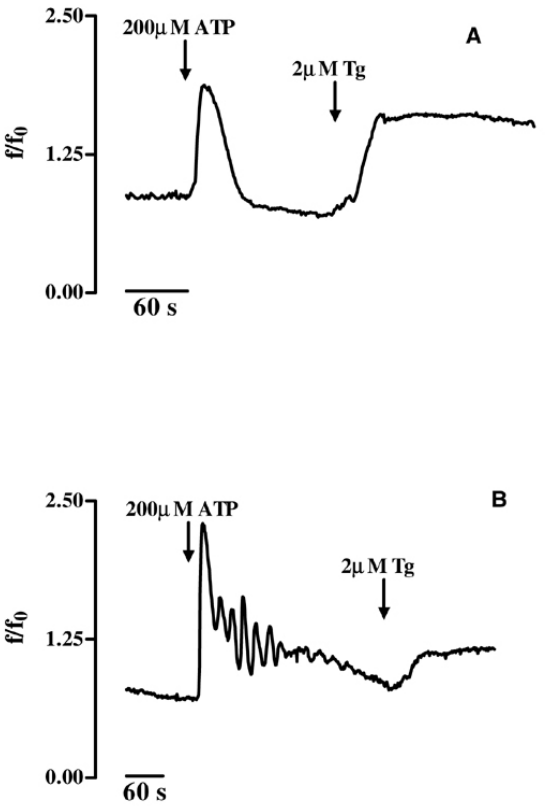

Figure 5

ATP-induced $[Ca^{2+}]_i$ variations in differentiated GL15 cells. Panel A shows a single Ca^{2+} spike induced by 200 μM ATP (arrow) in 32% of differentiated cells (n = 69); addition of 2 μM thapsigargin (Tg) (arrow) evoked a further increase in $[Ca^{2+}]_i$. In 18% (12 out of 69) of differentiated cells, 200 μM ATP (arrow) induced Ca^{2+} oscillations, partially inhibiting the thapsigargin-induced Ca^{2+} increase (B). Time (s=seconds) is indicated on the abscissa; the ordinate gives the normalized fluorescence value (f/f_0).

extracellular, receptor-mediated, chemical signal transduction (i.e. neurotransmitters - or stimuli triggered by growth factors), but also the gap junction intercellular communication (GJIC).

In order to assess the astrocytic properties that are shared by the GL15 cell line, it was important to investigate their capacity to establish functional GJIC. To achieve this aim, functional, immunocytochemical and

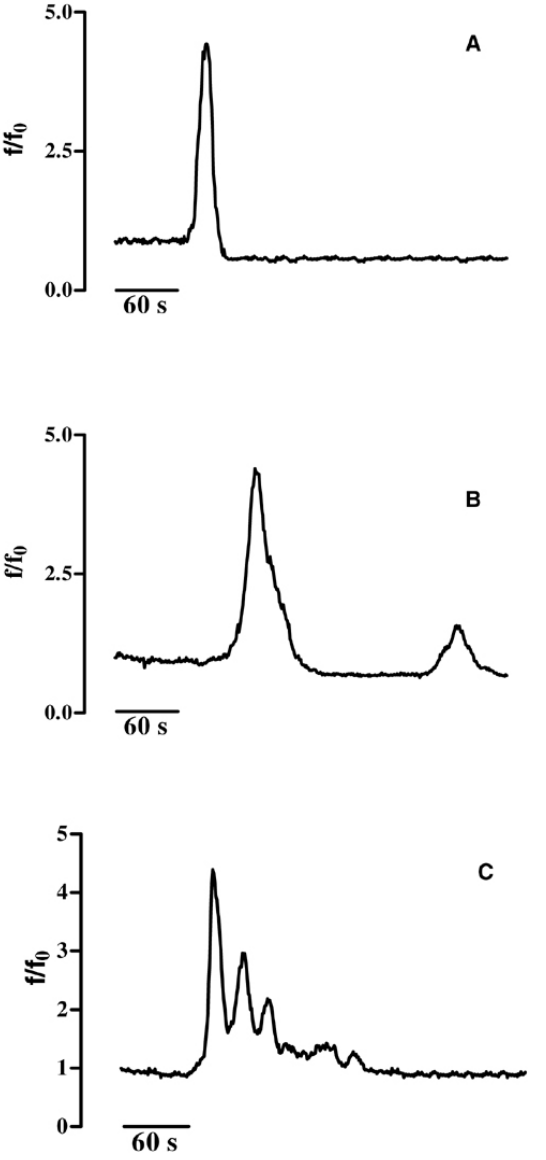

Figure 6

Spontaneous $[Ca^{2+}]_i$ variations in both undifferentiated and differentiated GL15 cells. Panels A, B and C show, respectively, a single $[Ca^{2+}]_i$ spike, low frequency $[Ca^{2+}]_i$ oscillations and high frequency $[Ca^{2+}]_i$ waves. 50% (n>200) of the cell population (differentiated or not) seemed to prime spontaneous intracellular Ca^{2+} movements. Time (s=seconds) is indicated on the abscissa; the ordinate gives the normalized fluorescence value (f/f_0).

molecular analyses were performed on GL15 phenotypes.

Table 2: Quantitative analysis of dye-coupling in GL15 cell cultures

GL15 cell cultures	n° of dye-coupled cells/ injection ± s.e.m. (n°)	% of communicating cells
undifferentiated sub-confluent	8.13 ± 0.74 (63)	100
undifferentiated confluent	3.91 ± 0.42 (64)	48.09
differentiated confluent	1.59 ± 0.25 (59)	19.55

The communication capacity of GL15 cells was quantified by counting the number of fluorescent cells surrounding the microinjected ones (n° of dye-coupled cells/injection) ± s.e.m.; n° = number of independent microinjections.

i) Functional analysis of GL15 junctional coupling. A microinjection/dye-transfer assay was employed to determine GJIC strength in differentiated and undifferentiated GL15 monolayers, analysed at different culture densities. Cells from undifferentiated, proliferating (sub-confluent) monolayers were clearly shown to be junctionally coupled. When the saturation density (confluence) of the cultures was reached, a significant reduction of the cell coupling was observed (48% of the value found in the proliferating counterpart). In the case of differentiated, resting GL15 cells (confluent cultures), dye-transfer was almost completely restricted to the cells initially loaded with the dye (Table 2). The GJIC capacity of GL15 cultures is shown in Fig. 7.

ii) Immunocytochemical analysis of connexin 43 (cx43) in GL15 cells. It is well known that cx43 is the main gap-junction protein expressed by astrocytes (both in vivo and in vitro); hence, its expression could have been responsible for the GJIC observed in GL15. The immunocytochemical localization of cx43 protein was performed by confocal microscopy on GL15 cultures kept in differentiating and proliferating conditions identical to those described above. The results showed the presence of the cx43 antigen in all the GL15 populations tested; however, the antigen distribution differed between populations, and its quantity was strictly related to the GJIC extent specific to each culture condition. In the highly communicating, sub-confluent, undifferentiated cells the punctate immunopositive reaction, typical of cx43 gjs aggregates, was localized close to the plasma membrane at cell-cell contact areas (Figs 8A and 8B; see also additional data: Movie 2 for the original data used to perform this analysis). The quantity gradually decreased when the cells reached the confluence status (Fig. 8C), and almost completely disappeared in the non-communicating, confluent differentiated GL15 cells (Fig. 8D). In all cases, randomly distributed cx43-positive staining was also found in the cytoplasmic compartment of GL15 cells. This could correspond to the unphosphorylated cx43 isoform that is usually defined as non-functional. Also in this case, an inverse relation was found between the GJIC capacity of the culture and the quantity of cx43 antigen located in the cytoplasm.

iii) Immunoblot analysis of cx43 in GL15 cells. The results of the immunoblot analysis of cx43 expression in the various GL15 cell populations (shown in Fig. 9), confirmed the results reported above. The anti-cx43 antiserum recognised, in control samples (rat heart and IAR 203 cell line), both the functional phosphorylated (44 and 47 kDa) and the unphosphorylated (42 kDa) isoforms of the connexin, whereas in GL15 cells only a small quantity of the 42 kDa antigen was detected. This observation may explain the very low communication capacity of this cell line. The quantity of the functional phosphorylated cx43 isoform could have been, in this case, under the limit of immunoblot sensitivity. Only in the samples of GL15 cells was an upper signal sized around 50 kDa detectable. This signal is probably due to a non-specific reaction of the anti-rabbit secondary antiserum with a protein only expressed by human cells. The possibility that it was caused by a slowly migrating, altered (and non-functional) isoform of cx43, typical of this cell line, is very unlikely. If this were the case, a very high total quantity of the cx43 antigen/single GL15 cell would be expected (much more than in the case of the IAR 203 cells, used as a positive control because of their extremely high cx43 expression level). However, the data obtained by the immunolocalization of the protein showed the quantity of cx43 antigen/single cell to be very low.

Discussion

The name glia - derived from the Greek word for glue - *per se* indicates why this cell compartment was considered the "less interesting element" of the nervous system until only a few years ago. Today the conception that researchers have of this cell population has completely changed, and, in general, theories concerning the role of astrocytes have been radically modified [19]. A recent, novel hypothesis put forward the possibility that this cell type is directly involved in the activity of brain tissue, and not just as a growth-factor producer. This hypothesis is strongly supported by the observation that astrocytes display rapid electrical responses to neuronal activity

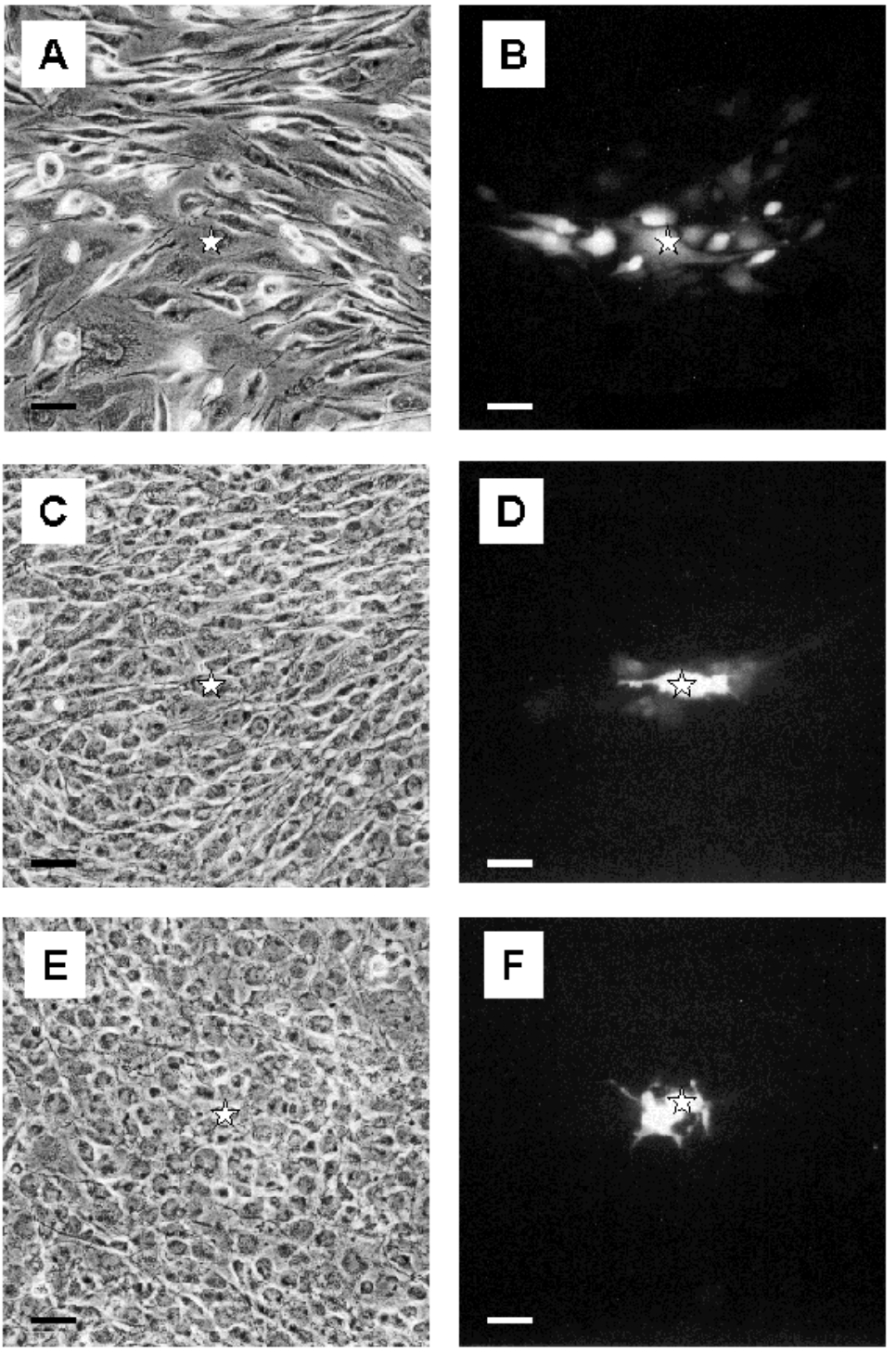

Figure 7
Pattern of dye coupling in GL15 cell cultures Sub-confluent monolayers of undifferentiated GL15 cells (A and B) show the presence of dye-permeant junctional channels. When the monolayers reached confluence (C and D), the dye-spreading capacity of the cells was reduced. Almost no dye spreading is observed in differentiated confluent GL15 cultures (E and F). Fluorescence (B, D and F) and the corresponding phase contrast (A, C and E) photographs are taken on formaldehyde-fixed cells, 15 min after dye injection. The star symbol indicates the microinjected cell. Bar = 50 μm.

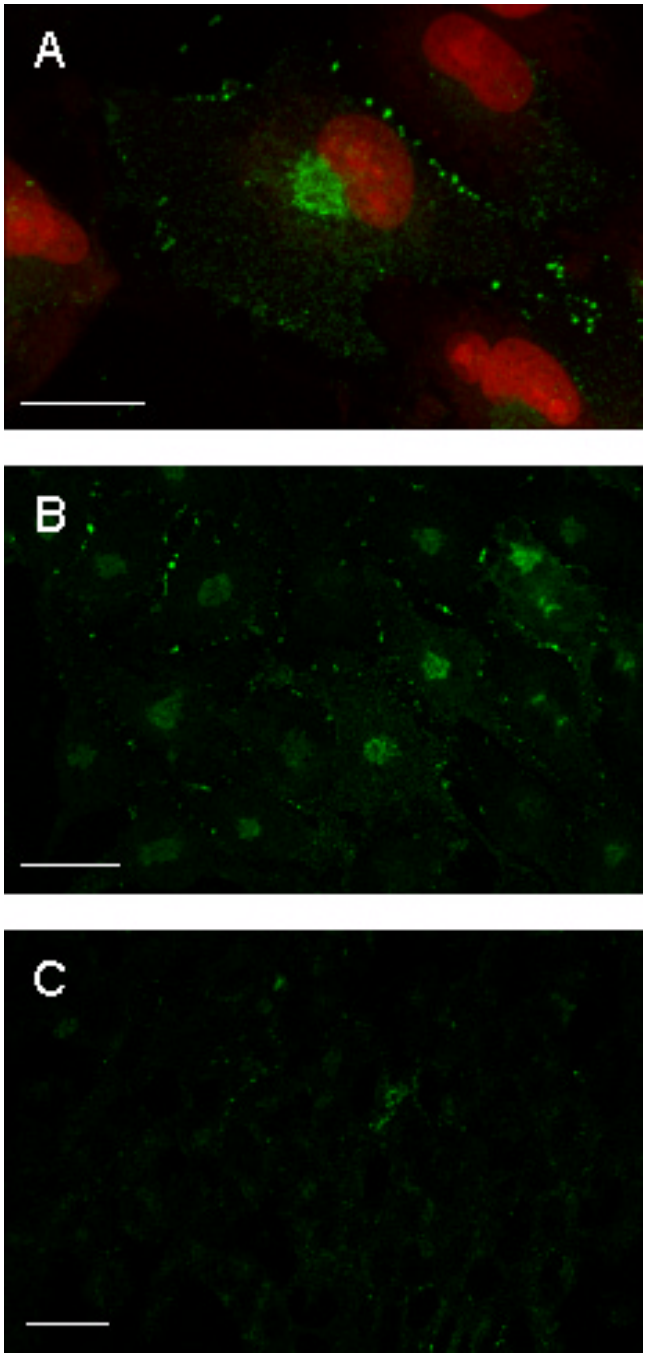

Figure 8
Expression of cx43 in GL15 cells. Confocal microscopy image acquisitions of cells stained with anti-cx43 antibody revealed by OregonGreen-conjugated anti-IgG. In panels A sub-confluent undifferentiated GL15 cells are also stained with Propidium Iodide. The image shown in A is an X-Y projection of a tri-dimensional reconstruction of 12 sections. Confluent undifferentiated GL15 cells (B) appear to poorly express cx43 in respect to sub-confluent undifferentiated cells (A). This feature was also observed in the confluent differentiated phenotype (C). Panels B and C represent a single focal plane at intermediate cell section. Bar = 25 μm.

and/or modifications of transductive systems [2, 4], like those of extracellular purines, which are known to be active in primary cultures of astrocytes [3].

Our experiments demonstrate that GL15 cells possess characteristics typical of astrocytes. The glial nature of this cell line was demonstrated by a number of experimental approaches, which collectively show that they have several astrocyte-like physiological properties. Immunostaining with anti-astrocyte protein-specific antibodies against GFAP and S100 showed the presence of specific glial markers GFAP and S100B, and the lack of the neuronal marker S100A, a particular isoform of S100 [17]. S100B and GFAP proteins were present in GL15 cultures, and the distribution pattern of S100B was relative to the differentiation status of the examined cells.

The presence of voltage-gated channels, correlated directly or indirectly with the possible generation of different transmembrane potentials, was indicated by data obtained from incubation of GL15 mature phenotype with 50 mM KCl, which induces membrane depolarisation. Under these conditions, a transient increase of $[Ca^{2+}]_i$ was observed, similar to that obtained in other excitable cells such as neurons, muscle cells or mature astrocytes [20]. By employing $[Ca^{2+}]_i$ variation as an indicator for the presence of Ca^{2+}-related receptors in these cells, it was further possible to demonstrate that the mature phenotype of GL15 cells is associated with different agonist-receptor systems. The presence of appropriate glutamate or ATP concentrations in the experimental medium induced significant $[Ca^{2+}]_i$ variation with specifc and agonist-related characteristics. However, upon testing with undifferentiated GL15 cells, these effects were either not present (i.e. ATP-induced $[Ca^{2+}]_i$ variation), or less marked (i.e. KCl-induced), or evident in a different way (i.e. L-glu-induced).

Our decision to examine $[Ca^{2+}]_i$ as probe for definitive astrocytic features of GL15 cells was based on the fact that the specific role played by astrocytes in many brain functions is achieved by Ca^{2+} signalling mechanism(s). Astrocytes express many different pathways, through which they react to external stimuli by variation of $[Ca^{2+}]_i$. In fact, these cells contain different forms of inositol triphosphate-coupled receptors that increase Ca^{2+} signalling, for example via the glutamate pathway and purine-activated systems. Ionotropic receptors, which open Ca^{2+} channels, are also found in this cell type. Furthermore, the presence of voltage-activated Ca^{2+} channels that permit Ca^{2+} fluxes from outside was demonstrated in both primary cultures and brain slices [4, 11].

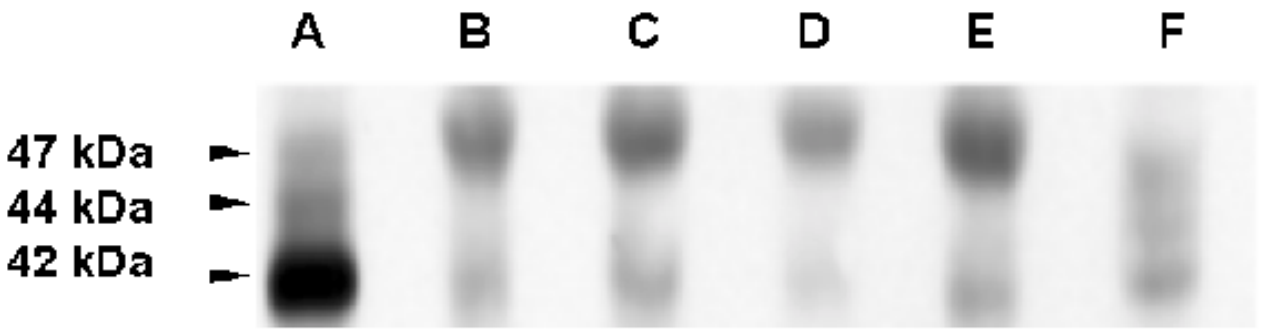

Figure 9
Immunoblot analysis of cx43 protein expression in GL15 cell line 40 μg of total protein extracts from undifferentiated and differentiated GL15 monolayers are electrophoresed and blotted according to Material and Methods. Normal rat heart and IAR 203 rat liver epithelial cells are included as positive controls for cx43 expression. Molecular-mass markers are shown in kDa. All the GL15 cultures express cx43. Note that, in both the rat heart and the IAR 203 samples, all the non-phosphorylated (42 kDa) and the phosphorylated (44 and 47 kDa) isoforms of cx43 are detected by the anti-serum. The protein extracts used for each lane are, (A) rat heart, (B) undifferentiated sub-confluent GL15 cells, (C) undifferentiated confluent GL15 cells, (D) differentiated sub-confluent GL15 cells, (E) differentiated confluent GL15 cells, and (F) IAR 203 cells. Results are representative of three immunoblots.

Therefore, it is well elucidated in the literature that the mechanisms involved in intracellular Ca^{2+} regulation (release from and uptake to Ca^{2+}-stores, capacitative and inductive Ca^{2+} currents, Ca^{2+} oscillations, and Ca^{2+} waves, etc) are present in astrocytes. If one considers that in these cells changes in $[Ca^{2+}]_i$ underlie a reciprocal communication system between neurons and astrocytes, assessing the presence and definition of the Ca^{2+}-system signalling in the GL15 cell line is fundamental in examining the reliability of this cell line as an astrocyte model.

All the Ca^{2+} pathways previously described for astrocytes are present in GL15 cells, although they are differentially regulated according to the differentiation status of the cell. It is possible to record oscillations in intracellular Ca^{2+} levels, generated either spontaneously or in the presence of ATP or Glutamate. On the other hand, depolarising agents like 50 mM KCl are unable to induce this phenomenon, which may therefore be considered independent from the voltage-operated Ca^{2+} channel status. This interpretation is credible, especially considering oscillating responses were also observed when extracellular Ca^{2+} was absent in the experimental medium. We hypothesise from the data that in the GL15 population, Ca^{2+} oscillations originate during Ca^{2+}-release from internal stores. The presence of a complete fan of receptor-operated responses in GL15 cells is correlated with the mature phenotype, whereas intercellular communication of astrocytes is associated with the immature status of GL15 cells. *In vivo*, astrocytes have the possibility to form 'functional syncytia' by establishing cytoplasmic connections through specific intercellular channels (gap junctions), which in turn provide pathways for the direct exchange of ions, small metabolites and water. Cultured astrocytes, like their *in vivo* counter-parts, are extensively coupled by gjs (cx43 being the predominant junctional protein expressed by these cells) [21].

Cx43 is expressed in specific brain regions by different glial populations like the other connexins (e.g. cx30), depending on the developmental stage of the tissue, different physio-pathological conditions and/or growth-factor influence [22, 23, 24].

Our results demonstrate that GL15 cells express the cx43 protein and form junctional channels in which permeability is directly related to the proliferation rate, and decreases when the differentiative status is reached.

The reduction of cell coupling when confluence is achieved supports the proposed role of GJIC in regulating astrocyte migration. In the differentiated phenotype, the very low levels of GJIC compared to that found in non-proliferating, undifferentiated confluent monolayers, demonstrated that even in a situation of 'mitotic arrest', factors other than those linked with cell-cycle progression (although probably dependent on the developmental features of the cells) may be involved in the regulation of GL15 cell coupling. These data confirm that physiologically, GL15 behave like glial cells with respect to both cell-cycle-dependent and differentiation-related regulation, and astrocytic junctional coupling (cx43 expression) [25]. A further point to note is that in the *in vit-*

ro conditions cx43 expression is limited to type I astrocytes [26].

It was observed that even when subjected to culture conditions allowing maximal junctional communication (sub-confluent, undifferentiated monolayer), the extent of GL15 dye-coupling was low, especially when compared to results obtained from other cultured cells of astrocytic origin [27]. This functional evidence closely reflects the data from immunocytochemical and immunoblot analyses, which indicate that in GL15 cells the junctional protein cx43 is expressed at low levels and its localization is mainly cytoplasmic, probably in the non-functional, unphosphorylated isoform. The presence of low levels of cx43 and limited intercellular coupling of GL15 cells is likely to be due to the neoplastic origin of this cell line, which is also observed in many other tumour-derived cell types such as C6 glioma cells [28]. Another possible explanation for the low communication capacity of GL15 cells might be the culture conditions. It has been demonstrated that the efficiency of junctional coupling of cultured astrocytes is positively influenced by interactions with other cell types (e.g. neurons and meningeal cells) [29, 30]. Moreover, in astrocytes (both *in situ* and *in vitro*), the different levels of dye-coupling (and cx43 expression) depend on factors such as the specific regional origin of these cells in the CNS or degree of maturation, thus suggesting that gjs formation in this cell type undergoes very complex environmental regulation [24].

Another important feature observed in our results was the correspondence between the modality of Ca^{2+} wave propagation in GL15 cells, and their GJIC capacity. Although several factors influence the extent of Ca^{2+} wave propagation, gjs permeability is a major determinant [11]. Heterogeneity in GJIC extent may, therefore, partly explain the heterogeneity of Ca^{2+} wave modulation and propagation in the GL15 population.

Conclusions

In conclusion, the data reported in this paper support the reliability of the GL15 cell line as a suitable *in vitro* model for astrocytes, which should aid in the investigation of their distinctive physiological properties, and subsequently contribute to clarifying the complex role of this cell type in the brain. It is important to remember that, by simply utilising the differentiated or undifferentiated phenotype of this cell line, it is possible to study the modality by which the cells communicate with each other, either via gjs and/or membrane receptors. The proposed model becomes even more fascinating when the human origin of this cell line is considered. This new astrocyte model provides a stepping-stone in the efficient analysis and interpretation of problems regarding the role of astrocytes during modulation and remodelling of the nervous system, their contribution to the electrophysiological activity of neurons and other relevant mechanisms.

Materials and Methods

Cell culture

GL15 cells were routinely cultured in growth medium (GM): D-MEM (Dulbecco's Modified Eagle's Medium) supplemented with 10% fetal calf serum (FCS), 100 IU/ml penicillin-100 μg/ml streptomycin and 2 mM L-glutamine. The cells were maintained at 37°C in a 5% CO_2 humidified atmosphere. The medium was changed twice weekly and the confluent cell monolayers were regularly sub-cultured, washing with phosphate-buffered solution (PBS) and treating with 0.5% trypsin-0.2% EDTA at 37°C for 5 minutes. Long-term differentiating cultures were obtained after a 10-day incubation of sub-confluent GL15 cultures in a differentiation medium (DM): D-MEM supplemented with 2% horse serum (HS), 100 IU/ml penicillin-100 μg/ml streptomycin and 2 mM L-glutamine. Undifferentiated cells were tested after a 1-2 day incubation in GM, while the differentiated phenotype was observed after culturing for 10 days in DM. All the experimental procedures were performed on cells of 60°-70° passage. All media, sera, antibiotics and culture solutions were purchased from Life Technologies Italia srl (S. Giuliano Milanese, Italy). Sterile culture plastics were purchased from Falcon (Plymouth, UK). All other reagents were of analytical grade purity.

Nuclear morphology

The cells were plated on 12 mm-glass coverslips (BDH Italia, Milano, Italy) at a density of approximately 2×10^4 cells/well and incubated in DM for 0, 3, 6, 9 and 12 days. At the selected times the cells were rapidly washed in PBS and fixed by 3.7% paraformaldehyde (Sigma, St. Louis, Missouri, USA) at room temperature (r.t.) for 15 minutes. The cells were then permeabilized with absolute methanol (Sigma) at r.t. for 5 minutes. After a single PBS washing, the samples were stained with 1 μg/ml 4',6-diamidino-2-phenylindole (DAPI; Molecular Probes, Eugene, Oregon USA) at r.t. for 5 minutes. After a double PBS washing, the coverslips were dried and mounted using a commercial mounting medium (Molecular Probes) and the DAPI fluorescence observed using an inverted Olympus IX 50 microscope (Olympus, Hamburg, Germany) equipped with an oil objective lens (Uapo/340 40X/1.35 oil Iris, Olympus). Regularly lobate nuclei were considered to belong to viable cells in cycle (indicated as normal); nuclei presenting two distinct lobes were considered to be in mitosis (indicated as mitotic), while enriched pluri-lobate nuclei were considered to be apoptotic. The quantification of each nuclear typology observed was represented by the percentage

mean ± s.d.. Each nucleus typology percentage was calculated from values derived from five randomly selected fields each containing about 50-60 cells on slices, in duplicate for each sample.

Fluorescence labelling and confocal microscopy

GL15 cells were grown on 12 mm-glass coverslips (plating density: 5×10^4 cells/well) as undifferentiated or differentiated cells. At the selected times the cells were rapidly washed with PBS and then fixed with 3.7% paraformaldehyde (Sigma) at r.t. for 5 minutes. The cells were then permeabilized with 0.1% Triton X-100 (Sigma) at r.t. for 5 minutes. These samples were used for fluorescent dye- or immuno-staining protocols. The dyes: Paclitaxel-Bodipy, Mitotracker-Green488, Propidium Iodide, Phalloidin-Alexa594 (all obtained from Molecular Probes) were used according to manufacturer's instructions. The immunolabelling procedure was preceded by 1 hour incubation of the cultures in 10% bovine serum albumin (BSA) at r.t.. Direct immunostaining detected the presence of GFAP, S100A and S100B proteins after 1 hour incubation (at 37°C) with the following antibodies, respectively: Cy3-conjugated mouse monoclonal anti-GFAP IgGs, Texas Red-conjugated mouse monoclonal anti-S100A IgGs, and Oregon Green-conjugated mouse monoclonal anti-S100B IgGs (all of these antibodies were obtained from Sigma and used at 1:100 dilution). Anti-S100A and anti-S100B were conjugated with their respective fluorochrome using FluoReporter Protein Labelling Kit (Molecular Probes). The presence of cx43 antigen was revealed by immunofluorescence: after 1 hour incubation at 37°C of the cells with primary mouse monoclonal anti-cx43 antibody (diluted 1:60) (Chemicon International Inc., Temecula, CA), followed by 1 hour incubation at 37°C with secondary Oregon Green-conjugated anti-mouse IgGs (diluted 1:100; Molecular Probes). The cells were washed 3 times for 5 minutes at r.t. with 0.1% Tween 20 (Sigma) in PBS, dried and then observed.

Fluorescence images were obtained by using a Bio-Rad MRC-1000 confocal system (BioRad Laboratories, USA) with an Axiovert 100 microscope equipped with a 63X/1.25 PLAN NEOFLUAR oil immersion objective lens (Zeiss, Jena, Germany). The Kr/Ar laser potency, photomultiplier and pin-hole size were kept constant for the entire experimental procedure. Images were acquired using CoMOS/MS-DOS software and then processed using LaserSharp/OS2 software (BioRad).

$[Ca^{2+}]_i$ measurements

GL15 cells were plated on 25 mm-glass coverslips at a density of 9×10^4 cells/well and tested as undifferentiated or differentiated cells. At the beginning of each experiment, the cells were washed with the normal external solution (NES), a buffered solution containing (in mM) 140 NaCl, 1.8 $CaCl_2$, 2.8 KCl, 2 $MgCl_2$, 10 Glucose and 10 HEPES/NaOH, at pH 7.4. The cells were then incubated for 30 minutes at 25°C with 3 μM Fluo3 acetoximethylester (Fluo3/AM, Molecular Probes) dissolved in NES supplemented with 10 mg/ml BSA. The loaded cells were rinsed and maintained for an additional 15 minutes at 25°C in NES to allow the complete de-esterification of the dye. In these experimental conditions each cell sample showed good preservation of the intracellular Ca^{2+} dye fluorescence emission. The coverslips were then transferred into an Attofluor chamber (Molecular Probes). Stimulating agents were added in less than 1 second to the cells kept at r.t.. A high-speed wavelength switcher Polychrome II (Till Photonics, Germany) equipped with a 75 W stabilised Xenon lamp (Ushio Inc., Japan) provided the excitation beam. The Polychrome II was connected to an Olympus IX 50 microscope equipped with an oil objective lens (Uapo/340 40X/1.35 oil Iris). The fluorescence emission was acquired by C6790 Hamamatsu camera and analysed using the Argus Hisca 1.7 software (Hamamatsu, Hamamatsu, Japan). The traces in Figs 3,4,5,6 were ratios (1 ratio/second) calculated off-line as f/f_0, where f is the fluorescence emission of a single FLUO3-loaded cell at time range from 1 to *x* seconds and f_0 is the fluorescence emission of the same cell at time 0 [31].

Dye-Transfer Assay

Undifferentiated (sub-confluent and confluent) and differentiated (confluent) GL15 cells, cultured onto 60-mm Petri dishes, were tested for their capacity to establish functional gjs as described by Mazzoleni et al. [32]. Briefly, single cells within the monolayers of three separate dishes were microinjected with a 10% (wt/vol) solution of the gap-junction-permeant fluorescent tracer Lucifer Yellow CH (Sigma) in 0.33 M LiCl. Microinjections were performed using glass capillary needles (Clark Electromedical Instruments, Edenbridge, UK), prepared with an automatic puller (Narishige, Tokyo, Japan) and driven by a Narishige micromanipulator (SYF II) linked to an Olympus IMT2 microscope. The fluorescent dye was injected under nitrogen pressure using an Eppendorf microinjector (Hamburg, Germany). Five minutes after the last injection, the cells were fixed with 4% paraformaldehyde in PBS and the dye-transfer capacity of the cells was observed using the IMT2 epifluorescence system. The extent of gap junction intercellular communication (GJIC) was then quantified by counting the number of fluorescent cells surrounding the microinjected ones (n° of dye-coupled cells/injection). At least 25 independent microinjection trials/dish were taken into account for the precise quantification of the GJIC competence of the culture. Data were expressed as mean ± s.e.m.. Bright-

field and fluorescence images were taken on Kodak T-MAX 400 (400 ASA) films.

Immunoblot analysis

Cells from six 100-mm Petri dishes were pooled for each previously described culture condition and the whole-cell extracts (40 μg protein of total lysate/lane) were first resolved by electrophoresis on 10% sodium dodecyl sulphate-polyacrylamide gel [33] and then transferred onto a nitrocellulose membrane (Schlesher and Shuell, Keene, NH). Protein of total lysate from rat heart and IAR 203 rat liver epithelial cells [34] were included as positive controls for cx43 expression. Total protein concentration was determined using a Bio-Rad DC Protein Assay kit (Bio-Rad, Segrate, Italy); equal sample protein-loading was verified by Comassie Blue staining of identical gels run in parallel, using a 0.25% Comassie Blue solution (R 250/G 250 1:1) (Bio-Rad). Membranes were hybridized with polyclonal rabbit anti-cx43 antibody (1:1000) (Chemicon International Inc.), followed by reaction with peroxidase-conjugated anti-rabbit IgGs (1:2000) (Amersham Pharmacia Biotech Italia, Cologno Monzese, Italy). Immunopositive reaction was detected by the enhanced chemiluminescence method (ECL, Amersham Pharmacia Biotech Italia) and revealed using autoradiography films (Hyperfilm-ECL, Amersham Pharmacia Biotech Italia).

Additional material

Structural and functional GL15 characteristics

To better visualise the structural and functional GL15 characteristics, we also include two movies in which it is possible to observe: Movie 1: A representative experiment showing spontaneous intracellular Ca2+ oscillations. Each frame was acquired with a ratio of 1 frame/second. The total number of frames was 120 with a total real time of 120 seconds compressed in the 30 seconds of the movie. Size bar = 50 μm.

Movie 2: Tri-dimensional reconstruction of cx43-immunostained undifferentiated GL15 cells. Size bar = 25 μm.

Movie 1
[http://www.biomedcentral.com/content/supplementary/1472-6793-1-4-S1.mov]
Movie 2
[http://www.biomedcentral.com/content/supplementary/1472-6793-1-4-S2.mov]

Acknowledgements

We wish to thank Dr Francesca Rovetta for helpful discussions and Peter A. Mattei for his assistance in preparing the manuscript. This work was supported by research grants from MURST-Italy (Ministero dell'Università e della Ricerca Scientifica e Tecnologica) to G.F. and from the University of Brescia to G.M.

References

1. Barres BA, Reichardt LF: **Neuronal and glial cell biology. Editorial overview.** *Curr Opin Neurobiol* 1999, **9**:513-516
2. Vesce S, Bezzi P, Volterra A: **The highly integrated dialogue between neurons and astrocytes in brain function.** *Sci Prog* 1999, **82**:251-270
3. Centemeri C, Bolego C, Abbracchio MP, Cattabeni F, Puglisi L, Burnstock G, Nicosia S: **Characterization of the Ca2+ responses evoked by ATP and other nucleotides in mammalian brain astrocytes.** *Br J Pharmacol* 1997, **121**:1700-1706
4. Carmignoto G, Pasti L, Pozzan T: **On the role of voltage-dependent calcium channels in calcium signaling of astrocytes in situ.** *J Neurosci* 1998, **18**:4637-4645
5. John GR, Scemes E, Suadicani SO, Liu JS, Charles PC, Lee SC, Spray DC, Brosnan CF: **IL-1 beta differentially regulates calcium wave propagation between primary human fetal astrocytes via pathways involving P2 receptors and gap junction channels.** *Proc Natl Acad Sci U SA* 1999, **96**:11613-11618
6. Finkbeiner S: **Calcium waves in astrocytes-filling in the gaps.** *Neuron* 1992, **8**:1101-1108
7. Smith SJ: **Neural signalling. Neuromodulatory astrocytes.** *Curr Biol* 1994, **4**:807-810
8. Sauer H, Hescheler J, Wartenberg M: **Mechanical strain-induced Ca2+ waves are propagated via ATP release and purinergic receptor activation.** *Am J Physiol Cell Physiol* 2000, **279**:C295-C307
9. Nedergaard M: **Direct signaling from astrocytes to neurons in cultures of mammalian brain cells.** *Science* 1994, **263**:1768-1771
10. Zhang W, Couldwell WT, Simard MF, Song H, Lin JH, Nedergaard M: **Direct gap junction communication between malignant glioma cells and astrocytes.** *Cancer Res* 1999, **59**:1994-2003
11. Giaume C, Venance L: **Intercellular calcium signaling and gap junctionalcommunication in astrocytes.** *Glia* 1998, **24**:50-64
12. Bocchini V, Casalone R, Collini P, Rebel G, Lo Curto F: **Changes in glial fibrillary acid protein and karyotype during culturing of two cell lines established from human glioblastoma multiforme.** *Cell Tissue Res* 1991, **265**:73-81
13. Arcuri C, Tardy M, Rolland B, Armellini R, Menghini AR, Bocchini V: **Glutamine sinthetase gene expression in a glioblastoma cell line of clonal origin: regulation by dexamethasone and dibutyryl cyclic AMP.** *Neurochem Res* 1995, **20**:1133-1139
14. Scarpa S, Coppa A, Ragano-Caracciolo M, Mincione G, Giuffrida A, Modesti A, Colletta G: **Transforming Growth Factor beta regulates differentiation and proliferation of human neuroblastoma.** *Exp Cell Res* 1996, **229**:147-154
15. Tchoumkeu-Nzouessa GC, Rebel G: **Characterization of taurine transport in human glioma GL15 cell line: regulation by protein kinase C.** *Neuropharmacology* 1996, **35**:37-44
16. Castigli E, Arcuri C, Giovagnoli L, Luciani R, Giovagnoli L, Secca T, Gianfranceschi GL, Bocchini V: **Interleukin-1β induces apoptosis in GL15 glioblastoma-derived human cell line.** *Am J Physiol Cell Physiol* 2000, **279**:C2043-C2049
17. Fanò G, Biocca S, Fulle S, Mariggio MA, Belia S, Calissano P: **The S-100: a protein family in search of a function.** *Prog Neurobiol* 1995, **46**:71-82
18. Thastrup O, Cullen PJ, Drobak BK, Hanley MR, Dawson AP: **Thapsigargin, a tumor promoter, discharges intracellular Ca2+ stores by specific inhibition of the endoplasmic reticulum Ca2+ ATPase.** *Proc Natl Acad Sci USA* 1990, **87**:2466-2470
19. Travis J: **Glia: the brain's other cells.** *Science* 1994, **266**:970-972
20. Armstrong CM, Hille B: **Voltage-gated ion channels and electrical excitability.** *Neuron* 1998, **20**:371-380
21. Zahs KR: **Heterotypic coupling between glial cells of the mammalian central nervous system.** *Glia* 1998, **24**:85-96
22. Ochalski PA, Sawchuk MA, Hertzberg EL, Nagy JI: **Astrocytic gap junction removal, connexin43 redistribution, and epitope masking at excitatory amino acid lesion sites in rat brain.** *Glia* 1995, **14**:279-294
23. Reuss B, Unsicker K: **Regulation of gap junction communication by growth factors from non-neural cells to astroglia: a brief review.** *Glia* 1998, **24**:32-38
24. Nagy JI, Rash JE: **Connexins and gap junctions of astrocytes and oligodendrocytes in the CNS.** *Brain Res Brain Res Rev* 2000, **32**:29-44

25. Bittman K, Owens DF, Kriegstein AR, LoTurco JJ: **Cell coupling and uncoupling in the ventricular zone of developing neocortex.** *J Neurosci* 1997, **17**:7037-7044
26. Belliveau DJ, Naus CC: **Cortical type 2 astrocytes are not dye coupled nor do they express the major gap junction genes found in the central nervous system.** *Glia* 1994, **12**:24-34
27. Giaume C, McCarthy KD: **Control of gap-junctional communication in astrocytic networks.** *Trends Neurosci* 1996, **19**:319-325
28. Naus CC, Bechberger JF, Caveney S, Wilson JX: **Expression of gap junction genes in astrocytes and C6 glioma cells.** *Neurosci Lett* 1991, **126**:33-36
29. Fischer G, Kettenmann H: **Cultured astrocytes form a syncytium after maturation.** *Exp Cell Res* 1985, **159**:273-279
30. Anders JJ, Salopek M: **Meningeal cells increase in vitro astrocytic gap junctional communication as measured by fluorescence recovery after laser photobleaching.** *J Neurocytol* 1989, **18**:257-264
31. Mammano F, Canepari M, G Capello, RB Ijaduola, A Cunei, L Ying, F Fratnik, A Colavita: **An optical recording system based on a fast CCD sensor for biological imaging.** *Cell Calcium* 1999, **25**:115-123
32. Mazzoleni G, Telo P, Camplani A, Tanganelli S, Monarca S, Ragnotti G: **Influence of the herbicide Linuron on growth rate and gap-junctional intercellular communication of cultured endothelial cells.** *J Environ Pathol Toxicol Oncol* 1994, **13**:1-10
33. Laemmli UK: **Cleavage of structural proteins during the assembly of the head of bacteriophage T4.** *Nature* 1970, **227**:680-685
34. Montesano R, Drevon C, Kuroki T, Saint Vincent L, Handleman S, Sanford KK, DeFeo D, Weinstein IB: **Test for malignant transformation of rat liver cells in culture: cytology, growth in soft agar, and production of plasminogen activator.** *J Nat. Cancer Inst* 1977, **59**:1651-1658